Surface functionalization of bioactive glasses and hydroxyapatite with polyphenols from organic red grape pomace

Received: 23 November 2020 | Revised: 9 March 2021 | Accepted: 1 April 2021

DOI: 10.1111/jace.17849

Journal of the American Ceramic Society

SPECIAL ISSUE ARTICLE

Surface functionalization of bioactive glasses and hydroxyapatite with polyphenols from organic red grape pomace

Giacomo Riccucci[1] | Martina Cazzola[1] | Sara Ferraris[1] | Virginia Alessandra Gobbo[1] | Marta Miola[1] | Antonella Bosso[2] | Gissur Örlygsson[3] | Chuen How Ng[4] | Enrica Verné[1] | Silvia Spriano[1]

[1]Politecnico di Torino, Turin, Italy

[2]Consiglio per la ricerca in agricoltura e l'analisi dell'economia agraria—Centro di Ricerca Viticoltura ed Enologia, Asti, Italy

[3]Innovation Center Iceland, Reykjavík, Iceland

[4]Genis hf, Siglufjördur, Iceland

Correspondence
Silvia Spriano, Politecnico di Torino, Corso Duca degli Abruzzi 24, 10129 TORINO, Italy.
Email: silvia.spriano@polito.it

Funding information
Seventh Framework Programme, Grant/Award Number: NAT4MORE; European Commission; MIUR

Abstract

An extract of polyphenols was obtained from organic red grape pomace, chemically analyzed, and used for functionalization of two bioactive glasses and porous hydroxyapatite. Functionalization is effective on hydroxyapatite and the bioactive glass with higher surface reactivity with a different grafting mechanism. Grafting does not inhibit redox and radical scavenging activity of polyphenols. The grafted polyphenols make a continuous layer with an almost complete surface coverage. Polyphenols are released with different kinetics according to the mechanism of grafting and maintain their redox activity. A homogeneous thin layer of polyphenols is still firmly grafted on both substrates after 28 days of soaking and it still maintains radical scavenging activity. The functionalized samples can be sterilized by gamma irradiation.

KEYWORDS

bioactive glass, hydroxyapatite, polyphenols, surface modification

1 | INTRODUCTION

The aim of this research was to obtain multifunctional bioactive ceramics and glasses for bone implants by combining inorganic materials and organic biomolecules grafted on them.

Bioactive glasses and hydroxyapatite were selected as substrates for grafting because these are both well-known to promote healing and to bond to bone and collagenous tissues through different bioactive actions. At first, bioactivity is related to the formation of a hydroxycarbonate apatite (HCA) layer on the glass surface after contact with biological fluids (e.g., blood plasma). HCA forms through a series of chemical reactions which occur within min to h after implantation.[1] Furthermore, bioactive glasses are bioactive because these have osteoinductive behavior promoting differentiation into an osteoblastic phenotype, encouraging the formation of bone matrix and getting an optimal mineralization of the tissue.[2] As implants, bioactive glasses are mainly used to restore interfaces or to fill a cavity.[3]

Hydroxyapatite, as the main inorganic component of bone, has long been known to be a biocompatible and osteoconductive ceramic material. Upon *in vivo* implantation in bone, a hydroxyapatite layer is precipitated on its surface leading to a chemical bond with the bone.[4] Furthermore, hydroxyapatite is bioactive because of the tight interplay with collagen fibrils and newly formed hydroxyapatite.[5]

Polyphenols (mixture of phenolic acids and flavonoids) were selected as biomolecules to be grafted because these are well-known for anti-inflammatory and -oxidant actions[6]; these are active both for the protection and formation

of biological tissues. In the case of bone, polyphenols can counteract the shift toward osteoclastogenesis in bone-loss pathologies[7] and are effective on osteoblasts through different signaling pathways.[8] There is clinical evidence that polyphenols have beneficial effects preventing the destruction of the gingival connective tissue and alveolar bone occurring in case of periodontitis[6,8] an inflammatory disease of polymicrobial origin affecting 30% of adults.[9] Polyphenols are characterized by important anti-inflammatory properties and redox activity through the numerous OH groups exposed on the aromatic rings.[10]

In this research, polyphenols are extracted from an organic red grape pomace because the winemaking byproducts (grape skins and seeds) are one of the richest sources of natural phenolic compounds.[9] The specific goal of this research was the addition of polyphenols to ceramic and bioactive glasses and chemical characterization of the functionalized materials. In the final application, these materials are of interest for local action (anti-oxidant, -bacterial, -viral, -allergic, -inflammatory effects) on the surrounding tissues after implantation. Two bioactive glasses with different reactivity and sintered hydroxyapatite have been considered as substrates. The type of chemical bond between the grafted polyphenols and the substrates is also investigated. In case of physical adsorption or weak electrostatic interaction, fast release (within some h) in the surrounding tissues and physiological fluids can be expected, while moving toward covalent or strong electrostatic bonds slow release (several days) can be expected. This is of relevance because the biological activity of the functionalized implants can be based on a release mechanism or a direct contact mechanism with the cells.

2 | MATERIALS AND METHODS

2.1 | Samples preparation

The names of all the samples and solutions are reported in Table 1. Two silica-based bioactive glasses were used: The composition of SCNA or A (Table 1) is given as: 57.0% mol SiO_2, 6.0% mol Na_2O, 34.0% mol CaO, and 3.0% mol Al_2O_3,[11] whereas the composition of SCNB or B (Table 1) is given as: 55.6% mol SiO_2, 22.7% mol Na_2O, and 21.7% mol CaO. Glass bars (10 mm diameter) were obtained by the melt and quenching process in a platinum crucible at 1550°C for 1 h for SCNA and at 1450°C for 2 h for SCNB. The melt was cast into a cylindrical brass mold preheated at the temperature of the annealing: SCNA was annealed at 600°C for 10 h and SCNB at 520°C for 6 h. The bars were cut in slices 2-mm thick with a diamond blade (IsoMet High Speed Pro,

TABLE 1 Table of acronyms and their descriptions

Name and description	Acronym	Characterization techniques
Hydroxyapatite	H	*UV-Vis spectroscopy, F&C test, DPPH test, Zeta Potential, Fluorescence microscopy, XPS*
SCNA	A	*F&C test, DPPH test, Zeta Potential*
SCNB	B	*UV-Vis spectroscopy, F&C test, DPPH test, Zeta Potential, Fluorescence microscopy, XPS*
Freeze-dried extract of polyphenols	P	*Spectrophotometric analysis, HPLC, XPS*
Pomace Flour	PM	*Spectrophotometric analysis, HPLC*
Functionalizing solution	H_2O+P	*HPLC, F&C test, Zeta Potential*
Removal Solution	RemS	*HPLC*
Functionalized substrates with polyphenols	A+P, H+P, B+P	*UV-Vis spectroscopy**, *F&C test, DPPH test, Zeta Potential, Fluorescence microscopy**, *XPS**
Functionalized substrates after the release test in water	A+P28, H+P28, B+P28	*UV-Vis spectroscopy**, *F&C test**, *DPPH test**, *Fluorescence microscopy**
Functionalized substrates after sterilization	A+P_S, H+P_S, B+P_S	*UV-Vis spectroscopy**, *Fluorescence microscopy**
Uptake solutions of the solid samples	Uptake A, Uptake H, Uptake B	*F&C test*

*indicates that A samples were not characterized with the mentioned technique.

Buehler). Polishing was performed with abrasive SiC papers (120–4000 grit).

Hydroxyapatite ($Ca_{10}(PO_4)_6(OH)_2$ – called H) disks (12 mm diameter) were prepared from α-tricalcium phosphate (<53 μm, α-$Ca_3(PO_4)_2$) and tetracalcium phosphate (<53 μm, $Ca_4(PO_4)_2O$), both from Himed ltd., USA, at a molecular ratio of 2:1. The powders were mixed thoroughly, then excess water was added to the mixture and the slurry was kept overnight at 40°C to allow hydroxyapatite formation. The excessive water was dried out to obtain cakes that were ground into powdery form. 0.60 *g* of the powder was weighed and pressed at 1400 *N* force in a 13 mm diameter mold to obtain 2-mm-thick disks. The disks were placed on an aluminum oxide surface and sintered at 1200°C for 10 h to reach the desired consolidation.

2.2 | Glass surface activation

The surface hydroxyl groups of the bioactive glasses were exposed as explained in[12,13]: Washing in an ultrasonic bath once in acetone for 5 m, three times in ultrapure water, and drying at room temperature.

2.3 | Extraction of polyphenols from grape pomace

The fermented pomace of organic Barbera grapes was sampled at Tre Secoli winery (Mombaruzzo, AT, Italy) at racking off, after soft pressing (0.5 bar). The whole pomace (skins +seeds) was dried in a ventilated oven (48 h, 35°C), then milled (coffee grinder, 1 min) to obtain pomace flour (powder) (PM). The extraction of polyphenols was performed according to[14]: The PM was extracted with the mixture ethanol/water (1:1), with the extraction ratio 1:6 w/v flour/solvent (100 *g* flour in 600 ml solvent), in a shaking stirrer for 2 h at room temperature. The extract was centrifuged at 18°C for 20 min at 2880×*g* (Centrifuge 5810 R Eppendorf—Hamburg, Germany), then the supernatant was separated from the solid residue, and freeze-dried.

2.4 | Surface functionalization

The functionalizing solution (H_2O+P-Table 1) is made of freeze-dried polyphenols in ultrapure water with a concentration of 5.0 mg/ml[12,13] mixed for 1 h at room temperature in darkness. Each substrate was soaked in 5 ml of the functionalizing solution for 3 h at 37°C in darkness. The temperature and duration of the functionalization process were set according to[15] in order to avoid degradation of the polyphenols and excessive pH increase due to ion release by the substrates. The functionalized samples were washed twice in ultrapure water, dried at room temperature, and stored in darkness. The uptake solutions, at the end the functionalization process, were analyzed as explained in Table 1.

2.5 | Release test

Six functionalized samples, for each type of substrate, were submitted to a release test for 4 weeks. Each sample was immersed in 15 ml of ultrapure water in darkness for 28 days at 37°C. Ultrapure water was selected as a release medium in order to separate the release phenomenon from the bioactivity process. Soaking water was replaced at each experimental time (1-7 −14–28 days) and analyzed with the F&C test (Section 2.10). After 28 days, the samples were characterized as described in Table 1.

2.6 | Sterilization

The samples were packed and sterilized with gamma radiations at 25 kGy (standard sterilization for medical devices, Medical Device Directive) by Gammatom (Guanzate, Como, Italy); sterilization was monitored through a dosimeter, previously applied to the packaging.

2.7 | Detachment of polyphenols from the functionalized samples

Three samples of H+P were washed in a solution (5 ml) of 50% of ultrapure water and acetone in an ultrasonic bath for 10 m to detach the grafted polyphenols from the surface.[16] It is called removal solution (RemS - Table 1).

2.8 | Characterization of the polyphenolic extract

2.8.1 | Spectrophotometric analysis

The freeze-dried extract was dissolved in 3 ml methanol. Total anthocyanins, flavonoids, polyphenols, and flavans reacting with vanillin were determined by spectrophotometry[17] some details are reported in Data S1.

2.8.2 | Characterization of condensed tannins (phloroglucinolysis method) and quantification of flavan-3-ols monomers by HPLC

Phloroglucinolysis is the acid-catalyzed cleavage of the condensed tannins (proanthocyanidins) in the presence of excess

phloroglucinol as a nucleophile molecule.[18] The method consists of the phloroglucinolysis reaction and the HPLC analysis of the reaction products. The operating protocol is described in[9,19] The total condensed tannins content, their mean degree of polymerization (mDP), and the percentage of each constitutive unit were determined. Monomer flavan-3-ols ((+)-catechin and (–)-epicatechin) were determined with the same HPLC method used for the phloroglucinolysis method, excluding the reaction with phloroglucinol, as reported earlier; some details are reported in Data S1.

2.9 | UV-Vis spectroscopy

UV visible analyses were performed on solid samples by means of a UV-vis spectrophotometer (UV2600 Shimadzu equipped with the integrating sphere) in reflectance for hydroxyapatite and transmittance for the glasses. In the case of the liquid specimens, both the whole spectrum (250–700 nm) of the solutions and specific signals after the colorimetric tests (Folin&Ciocalteu, Section 2.10 and DPPH, Section 2.11) were measured.

2.10 | Total phenols by F&C test (Folin&Ciocalteu test)

The test, based on the evaluation of the absorbance of the wavelength at 760 nm through UV-Vis spectroscopy, was carried out to quantify the total phenols as Gallic Acid Equivalents (GAE).[20,21,22] The F&C reagent (Folin&Ciocalteu phenol reagent, Sigma-Aldrich) was used to carry out the test and the obtained solution was analyzed with UV-Vis spectroscopy after 2 h of reaction; some details are reported in Data S1.

2.11 | Radical scavenging activity by DPPH test

The DPPH test was performed following.[23] Each sample was placed in a dark container and soaked in 3 ml of the prepared DPPH solution at room temperature in darkness for 4 h. The measure of the absorbance was performed at 515 nm after 4 h; the same measurement was repeated after 24 h in accordance with.[24]

2.12 | Zeta Potential titration measurements

The zeta potential titration curves were measured with an electrokinetic analyzer (SurPASS, Anton Paar) on the solid samples. Two samples were put parallelly, at about 100 μm, and zeta potential was measured as a function of pH in a 0.001 M KCl electrolyte solution with an automatic titration unit. The same couple of samples was used both for the acidic (firstly) and basic (later) range, starting at pH 5.5 in both cases. Concerning the functionalizing solution, the zeta potential curve was obtained through the measurement of the electrophoretic mobility (Nanosizer Nano Z, Malvern Instrument, Malvern) changing pH step by step from pH 2.5 to 9 by adding HCl 0.05 M or NaOH 0.05 M.

2.13 | Fluorescence microscopy

Fluorescence microscopy was performed through a confocal microscope (LSM 900, ZEISS) equipped with a fluorescent light source and a red filter (573 nm); magnification was set at 200X and the exposure time at 1 s. Polyphenols autofluorescence is described in.[25,26]

2.14 | X-ray Photoelectron Spectroscopy (XPS)

Chemical analysis was performed by means of X-ray Photoelectron Spectroscopy (XPS, PHI 5000 VERSAPROBE, PHYSICAL ELECTRONICS). 400×400 μm areas were analyzed on each sample. Survey spectra were acquired between 0 and 1200 eV. High-resolution spectra of C, O, and Ca regions were acquired and referenced by setting the hydrocarbon C1 s peak to 284.80 eV (to guarantee the charging effect compensation).

3 | RESULTS

3.1 | pH variation during the functionalization processes

The pH value of the functionalizing solution (H_2O+P) is 3.6; it is stable during the functionalization process of SCNA, whereas pH increases to 5.7 in the uptake solution of hydroxyapatite (Uptake H) and to 4.6 for SCNB (Uptake B). The increase in pH of the uptake solutions of H and B (Uptake H and Uptake B) is due to surface reactivity and ion exchange ability of these substrates; it is less evident for A (Uptake A) due to the lower surface reactivity of this glass.

3.2 | Polyphenolic characterization of the pomace extract, functionalizing, and removal solutions

The total polyphenolic content (Table 2) refers to the dry weight (DW) of pomace flour (PM) (skins +seeds, milled)

and to the DW of the freeze-dried extract (P). The GAE index is the most used spectrophotometric parameter to evaluate the potential antioxidant properties. The total flavonoid index, based on the property of polyphenols to absorb at 280 nm—and the index of flavans reactive with vanillin, which expresses the concentration of low molecular weight tannins—were also determined by spectrophotometry. The monomer flavan-3-ols and the condensed tannins (or flavans, the polymeric forms of flavan-3-ols) were also quantified by HPLC. The most abundant compounds in the analyzed PM and freeze-dried extract are the condensed tannins (Table 2), whereas monomer flavan-3-ols only account for about 5% of the polymeric forms. The monomer units which compose the condensed tannins of grape skins and seeds are (+)-catechin,(−)-epicatechin,(−)-epicatechin-3-O-gallate and (−)-epigallocatechin[27]; the latter limited to the skin. (−)-epicatechin is the most abundant monomer unit and approximately 20% of the flavan-3-ols in tannins are esterified with gallic acid (galloylated form). The freeze-drying process increases the concentration of the polyphenolic compounds and the mean polymerization degree of the condensed tannins (mDP), which increases from 3.5 to 4.2 units. After freeze-drying, the percentage weight of the monomer units of the condensed tannins remains unchanged; a slight variation is observed in the percentage distribution of the different monomers between terminal and extension units, because of the increased size (mDP) of the flavanic chains.

TABLE 2 Polyphenolic composition (average values ± standard deviation, n = 3) of the grape pomace extract, referred to the dry weight (DW) of the pomace flour (skins + seeds, milled) and of the freeze-dried extract. mDP = mean degree of polymerization; G % = percentage of galloylation; EGC = (−)-epigallocatechin; C = (+)-catechin; EC = (−)-epicatechin; ECG = (−)-epicatechin-3-O-gallate

	Pomace flour (PM)	Freeze-dried extract (P)
Total polyphenols—GAE (mg/g)	7.3 ± 0.3	182 ± 16
Total anthocyanins (mg/g)	1.5 ± 0.03	35 ± 3
Total flavonoids (mg/g)	11.0 ± 0.10	200 ± 13
Flavans react. vanillin (mg/g)	2.1 ± 0.08	61 ± 2
mDP	3.5 ± 0.10	4.2 ± 0.07
G %	17.0 ± 0.20	18.4 ± 0.5
Condensed tannins (mg/g)	2.6 ± 0.07	95 ± 4.5
Principal monomeric units (%)		
EC	73.0 ± 1.12	71.2 ± 0.6
C	27.0 ± 1.12	28.8 ± 0.6
Extension units (%)		
EGC	0.94 ± 0.07	3.3 ± 0.2
C	14.3 ± 0.60	18.8 ± 0.5
EC	42.5 ± 1.18	39.3 ± 0.7
ECG	13.3 ± 0.22	14.9 ± 0.4
Terminal units (%)		
C	12.8 ± 0.54	10.0 ± 0.6
EC	12.5 ± 0.34	10.2 ± 0.2
ECG	3.7 ± 0.04	3.5 ± 0.1
Flavan−3-ols (mg/g)		
C	0.063 ± 0.01	1.72 ± 0.07
EC	0.077 ± 0.01	1.97 ± 0.07
ECG	traces	0.12 ± 0.03

The content of condensed tannins was evaluated in the functionalizing solution (before functionalization) (Table 3), as well as in a RemS (see Section 2.7); functionalized hydroxyapatite was selected to obtain RemS because of the highest amount of grafted polyphenols with respect to the glasses. Concerning the functionalizing solution, the mean degree of polymerization (mDP) drops from 4.2 to 2.9 units, and the galloylation degree (G%) from 18.4 to 15.9% with respect to the extract. Conversely, (−)-epicatechins remain the most abundant monomer unit and the percentage weight of C and EC remains unchanged. Concerning the RemS, the concentration of condensed tannins was modest compared to the functionalizing solution. The composition of condensed tannins varied with respect to the functionalizing solution: In particular, the percentage weight increased for (+)-catechin and decreased for (−)-epicatechin, whereas the

TABLE 3 Content and composition of condensed tannins in the functionalizing solution and in the removal solution from hydroxyapatite. mDP = mean degree of polymerization; G % = percentage of galloylation; C = (+)-catechin; EC = (−)-epicatechin; ECG = (−)-epicatechin-3-O-gallate

	Functionalizing solution (H_2O+P)	Removal Solution (RemS)
mDP	2.9	2.6
G %	15.9	7.4
Condensed tannins (mg/g)	15.3	1.9
Principal monomeric units (%)		
EC	70.3	47.8
C	29.7	52.2
Extention units (%)		
C	17.7	22.3
EC	37.0	31.4
ECG	11.3	7.4
Terminal units (%)		
C	12.0	29.9
EC	17.4	9.0
ECG	4.6	traces

galloylation degree (G%) was halved. The selective grafting of (+)-catechin is of interest because of stereospecificity of catechins in their biological activity that is also related to the degree of polymerization, molecular weight, and percentage of galloylation.[28] The mean polymerization degree (mDP) of the condensed tannins remained practically unchanged compared to that of the functionalizing solution.

3.3 | UV-Vis spectroscopy and F&C test of the functionalizing and uptake solutions

The analysis of the functionalizing and uptake solutions was also performed by UV-Vis spectroscopy (Figure 1.1). The amount of polyphenols grafted onto the substrate is negligible in comparison with the concentration of the functionalizing solution, making the difference after functionalization inconsiderable. Therefore, the up-take solutions are not reported in Figure 1.1. Two main peaks are visible in Figure 1.1: The first one (at 280 nm) corresponds to all polyphenols and is due to the aromatic ring,[29] whereas the second one at 530 nm belongs to anthocyanins at acidic pH.[22] The two overlapped peaks around 320 and 370 nm are characteristic of hydroxycinnamic acid[22] and quercetin (belonging to flavonols).[30] The results of the F&C test of the functionalizing and uptake solutions are compared in Figure 1.2. There are no significant differences before and after the functionalization process on the different substrates. It can be evidenced that the polyphenols are not altered despite the increase in pH.

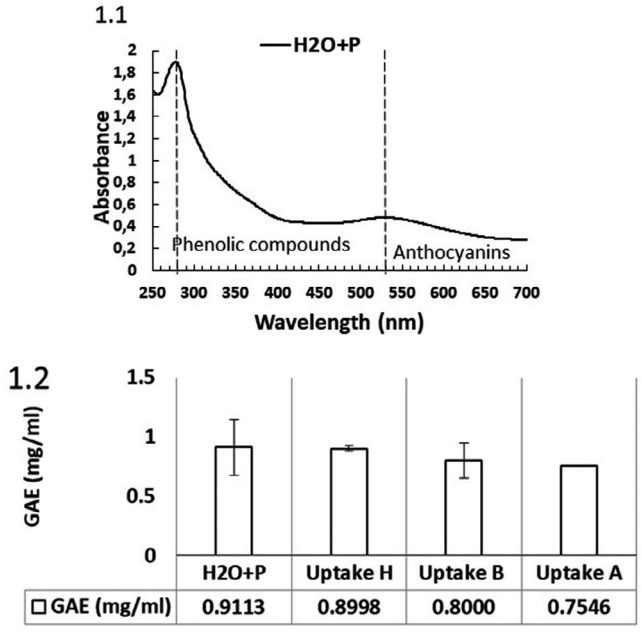

FIGURE 1 Characterization of the functionalizing solution through UV-VIS spectroscopy (1.1); results of the F&C test on the functionalizing and uptake solution (1.2)

It can be noted that the uptake solutions of the substrates A and H (Uptake A, Uptake H) have a lower standard deviation compared to the functionalizing solution and the uptake of the substrate B (Uptake B).

3.4 | F&C test on the solid samples and soaking water of the release test

The as-prepared substrates and a control solution (Control GAE) were analyzed as a reference (Figure 2). The null value on the control solution evidences no systematic error in the test (Figure 2). The first comparison is done among the bare substrates: GAE on A is zero, whereas H and B have a low chemical reducing ability. After the functionalization process, the increase in GAE on A+P (with respect to A) is not significant, whereas it clearly increases on H+P and on B+P (vs. H and B) (Figure 2). It means that the grafting of polyphenols to a bioactive glass is strictly connected to its surface reactivity and composition.[12,15,31,32] The lower reactivity of A is due to alumina which increases the stability of the bioactive glass.[33] Because of the low amount of grafted polyphenols on A, this substrate was not used for some further tests (such as the measure of GAE after the release test and sterilization). The positive outcome of the test on B + P and H + P evidences also that the grafted polyphenols maintain their chemical redox activity. The highest GAE value is appreciable on H + P as expected because of the high specific surface and surface reactivity of this porous ceramic.

The GAE was measured also on H + P28 and B + P28: These are the functionalized samples after 28 days of soaking in water. The GAE values show after soaking a clear decrease down to the value of the as-prepared substrates (H and B). The soaking water of each sample was analyzed by the F&C test after 1, 7, 14, and 28 days of the release test (Table 4). Concerning H + P, there is a slow release of polyphenols at 1, 7, and 14 days, with low values of GAE registered in the soaking water. However, the release occurs mainly with longer times with a high value of GAE registered at the end of the release test (28 days). Differently, B + P has a quick release of polyphenols into the water during the first day, then the release remains very low and constant during the subsequent 2 weeks, to increase again at 28 days. These results will be discussed in Section 3.5. The use of ultrapure water as a release medium allows to focus the attention on polyphenol release. Release test in SBF can lead to the simultaneous release of polyphenols and ions and hydroxyapatite precipitation making more difficult the final result interpretation. The release in more complex solutions can be considered as the future development of the work.

The value of GAE registered on the functionalized samples after sterilization was obtained (H+P_S and B+P_S—Figure 2) and it is analogous to the as functionalized samples

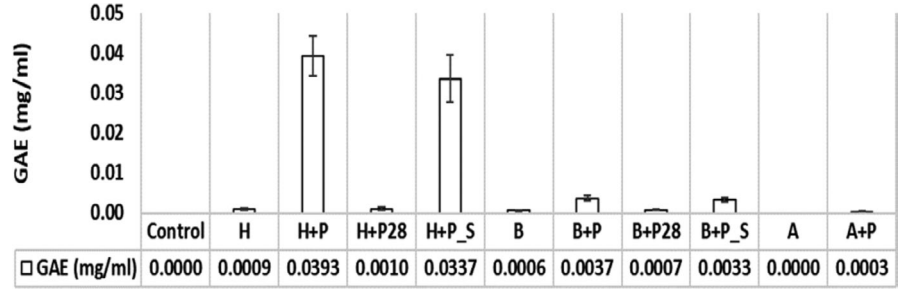

FIGURE 2 Results of the F&C test modified for the solid samples. GAE values measured on the control (Control GAE), unfunctionalized substrates (A, H, B) and functionalized (A+P, H+P, B+P) samples, as well as on the functionalized samples after the release test in water for 28 days f(H+P28, B+P28) or sterilization (H+P_S, B+P_S)

TABLE 4 GAE values measured on water after 1 day, 7 days, 14 days and 28 days of soaking of the H+P and B+P substrates

	GAE (mg/ml)			
	1 d	7 d	14 d	28 d
Control	0.0000	0.0000	0.0000	0.0000
Soaking water H+P	0.0002	0.0001	0.0003	0.0110
Soaking water B+P	0.0017	0.0001	0.0001	0.0015

(H+P and B+P), suggesting that grafted polyphenols maintain their redox activity after sterilization.

3.5 | DPPH test on substrates, functionalized samples, and after the release test

The scavenging activity of the hydroxyapatite substrate (sample H) is low even if not null. The elevated surface-to-volume ratio of the porous hydroxyapatite substrate allows to graft a high amount of polyphenols and it results in a high scavenging activity of the functionalized surface. Therefore, the RSA percentage increased over 80% on H+P (Figure 3). Finally, considering RSA as a function of time, it is also possible to appreciate how the antioxidant activity of the functionalized samples increases over time: The ability of polyphenols to scavenge the DPPH radicals is higher when evaluated after 24 h than after 4 h. The phenomenon is easily appreciated in H+P at 24 h.

Concerning substrate B, the radical scavenging activity of the as-prepared material is null (Figure 3), as the material does not show any activity. On the other hand, B+P (Figure 3) shows a significant antioxidant activity measured both after 4 and 24 h. The high RSA observed for H+P and B+P evidence that polyphenols maintain their scavenging activity also after grafting.

Both the RSA percentages of A and A+P are low: These do not reach 10% (Figure 3) and the scavenging activity, caused by the presence of polyphenols, is negligible, confirming the low amount of grafted polyphenols on this substrate already observed in the F&C test. This is the reason why the DPPH test is not performed on the sample A+P after release in water.

The high percentage of RSA of the samples soaked in water (H+P28 and B+P28) demonstrates that there is not a loss of scavenging ability after soaking in water on these functionalized surfaces. In the DPPH test performed at 24 h, H+P28 and B+P28 do not show differences in comparison to H+P and B+P, differently from the F&C results. The difference registered between the results of the F&C and DPPH tests performed on the samples after 28 days of release can be explained considering that the DPPH test is sensitive to the outermost surface layer of firmly grafted polyphenols. On the other hand, the F&C test, generally employed for redox compounds in liquid solutions and here adapted by the authors to the solid samples,[11,25] is mainly sensitive to the molecules adsorbed on the surface and released into the reagent during the test, rather than to the firmly grafted ones.

3.6 | Zeta Potential titration measurements

Zeta potential titration curves, as a function of pH, were acquired, respectively, on the polyphenols in an aqueous environment and on the investigated surfaces (Section 2.12); the two types of measurements were performed by different equipment, but the results can be compared. Zeta potential measurements give information on the isoelectric point, hydrophilicity, exposition of acid/basic functional groups, and surface chemical stability in contact with an aqueous environment at different pH, as explained in Data S1.

The presence of acidic functional groups in the polyphenols results in IEP at pH 2 of their solution (Figure 4.1), as obtained through interpolation of the curve. Along the zeta potential titration curve of the polyphenols, two changes in slope can be evidenced, one around pH 4 and the other around pH 6: these are caused by deprotonation of two types of OH groups, the carboxylic and the phenolic one, respectively. The former behaves as an acid stronger than the latter.

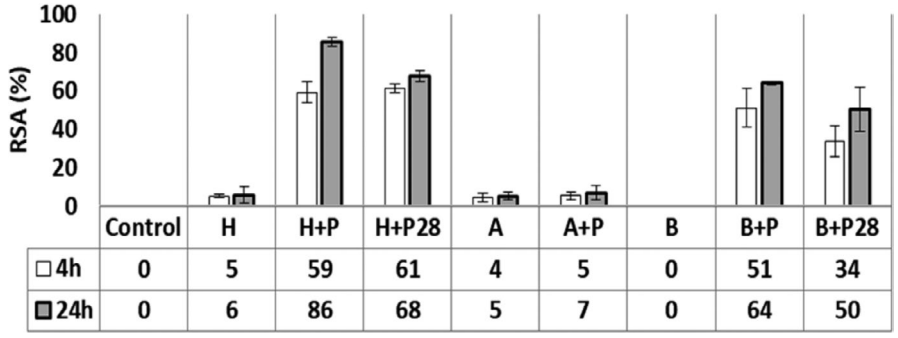

FIGURE 3 Radical scavenging activity measured through the DPPH test after 4 and 24 h from the beginning of the test: A control solution (Control DPPH), the unfunctionalized (A, H, B), functionalized samples (A+P, H+P, B+P), and the samples after the release test (H+P28, B+P28)

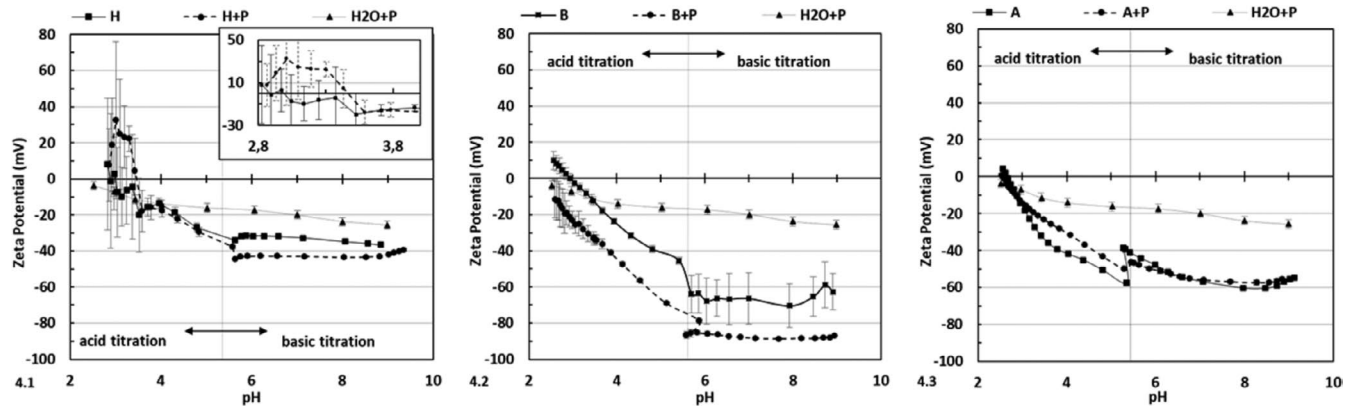

FIGURE 4 The zeta potential titration curves of the analyzed samples. (4.1) Hydroxyapatite before (H) and after functionalization (H+P) with a magnification of the acidic range. (4.2) SCNB before (B) and after functionalization (B+P). (4.3) SCNA before (A) and after functionalization (A+P). The curve of polyphenols in water (H2O+P) is reported in each figure as a reference

The zeta potential titration curves of H and H + P are compared (Figure 4.1). H has IEP at pH 3 and marked reactivity below pH 3.5, as it can be deduced from the high values of standard deviation. At pH higher than 5.5, there is a plateau at −35 mV: OH functional groups with acidic chemical reactivity (according to the low value of IEP) are completely deprotonated at pH 5.5 or higher. Concerning H+P, there is an increment of IEP up to pH 3.5 for H+P with respect to H (Figure 4.1). The standard deviation at acidic pH, always elevated, is nonetheless lower for H + P compared to bare H (as observable in the insert of Figure 4.1). It can be assessed that the surface zeta potential of H is not significantly changed by functionalization, but chemical stability in the acidic range is higher.

On the other side, the surface of B + P has zeta potential values lower than B at any pH (Figure 4.2). IEP is at pH 3.4 for B, while it is calculated, through interpolation of the curve, around 2 for B+P. Both the surfaces have a plateau with onset around pH 5.5. Furthermore, the high error bars of the curve of B indicate a high surface reactivity of B in the basic range. This phenomenon is avoided by the presence of polyphenols on the B+P surface, whereas on the contrary, the error bars become larger in the acidic range below pH 4. These results will be discussed in detail in Section 3.9.

A and A+P (Figure 4.3) have zeta potential titration curves with a very similar trend: No significant difference (equal or larger than 20 mV) in zeta potential can be detected. The IEPs of the substrate (A) and functionalized bioactive glass (A+P) differ only by of 0.1 (2.7 with respect to 2.6). Standard deviation is almost null at any pH, mainly because of the high chemical stability of A.

3.7 | Fluorescence microscopy

Fluorescence microscopy images are reported in Figure 5. H does not emit any red fluorescent signal, whereas H+P has an intense and homogeneous fluorescent signal (Figure 5.1, 5.2) due to autofluorescence of the grafted polyphenols. After 4 weeks of soaking in water (release test), there is a weak, but the uniform distribution of polyphenols on H+P28; the intensity of the red fluorescent signal decreases (Figure 5.3), and yellow and orange shades appeared on H+P28: It confirms that polyphenols are not completely released. Concerning H+P_S (Figure 5.4), there is not a significant change of the polyphenols layer both for the signal intensity and distribution because of sterilization.

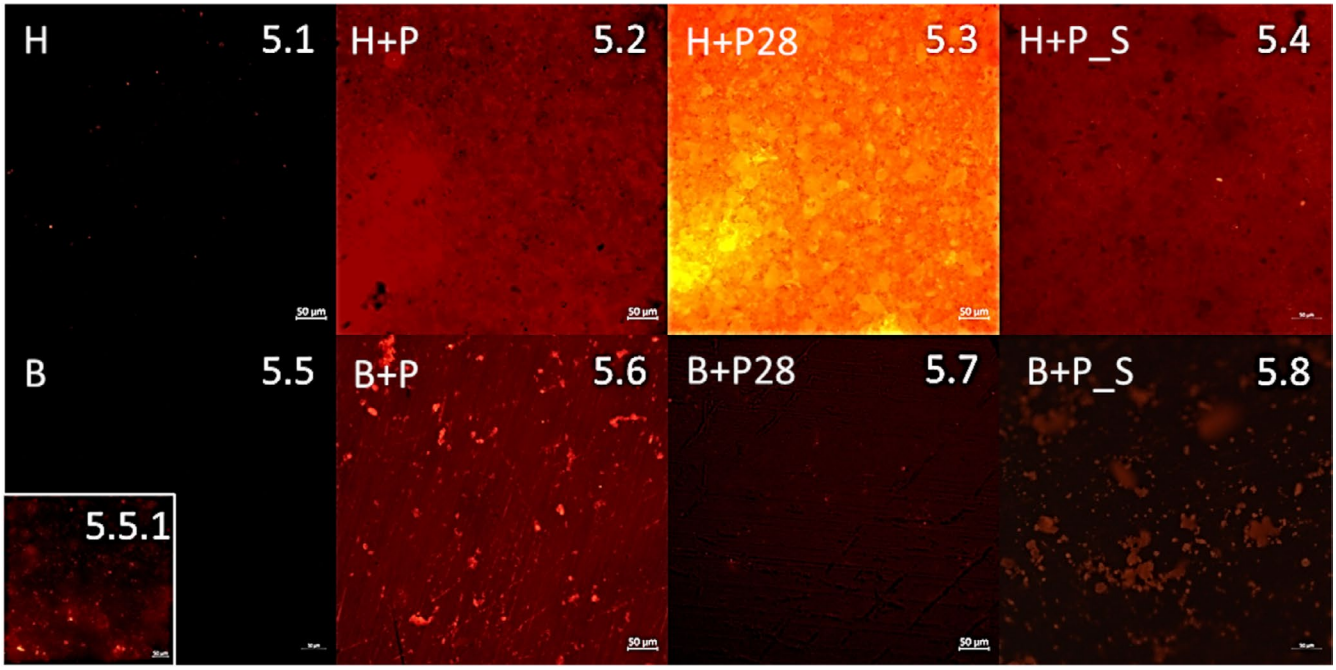

FIGURE 5 Red fluorescence images of the samples. (5.1) Hydroxyapatite (H); (5.2) functionalized hydroxyapatite (H+P); (5.3) functionalized hydroxyapatite after the release test in water (H+P28); (5.4) functionalized hydroxyapatite after sterilization (H+P_S); (5.5) SCNB after a controlled washing procedure (B); (5.5.1) SCNB after conventional washing (B); (5.6) functionalized SCNB (B+P); (5.7) functionalized SCNB after the release test in water (B+P28); (5.8) functionalized SCNB after sterilization (B+P_S)

In the case of substrate B (Figure 5.5, 5.6), it must be considered that B is naturally covered by a layer of carbonates here easily observable because of their fluorescent signal (Figure 5.5.1). The carbonates are formed in presence of water and CO_2[31] during conventional washing and drying of the glass surface (paragraph 2.2). A specimen of B was soaked in water for 3 h at 37°C and quickly dried with compressed air, to avoid the formation of carbonates: This sample can be used as a control glass surface without carbonates[32] (Figure 5.5, 5.5.1). The amount of grafted polyphenols on B+P (Figure 5.6) is significant as derived from the high fluorescent signal. There are both red (dark) diffused signal and large bright spots showing the presence of both a continuous layer and agglomerates of polyphenols on the surface. It can be supposed that the formation of a layer of silica gel on the surface of this bioactive glass during soaking in an aqueous environment plays a role in the grafting mechanism of a continuous layer of polyphenols on this substrate (Section 3.9). The supposed formation of the layer of silica gel (hydrated layer) is coherent with the FTIR-ATR peak at 900–500 cm^{-1} observable on B + P28 sample, after soaking in water (Data S1). Soaking in water for 28 days induces a complete release of the polyphenols agglomerates. In fact, there is no more large bright red spot on B+P28. The dark red diffused signal is attenuated, but still visible on B+P28 confirming that a layer of polyphenols is still grafted after soaking. About B+P_S (Figure 5.8), there is a decrease in the fluorescence intensity, especially concerning the continuous layer: Polyphenols grafted on B are a bit less stable to sterilization than on H.

3.8 | UV-VIS spectroscopy of the solid samples

The UV-Vis spectra of H, H+P, H+P28, and H+P_S are shown in Figure 6.1. The reflectance of H is high and it has a plateau in the range 450–700 nm, whereas it progressively decreases in the range 250–400 nm. On the other hand, H+P has a very low reflectance up to 600 nm: The presence of a glare-free coating due to the grafted polyphenols is evident. H+P and H+P_S have comparable UV-Vis spectra. H and H+P28 are characterized by similar, even if not identical reflectance (a lower reflectance of H+P28 is observable), confirming the release of a part of polyphenols.

The sample B has an elevated percentage of transmittance in the visible range, as expected for transparent material; from 400 nm toward lower wavelengths, transmittance decreases (Figure 6.2). The same trend is followed by B+P, and B+P_S, but presenting lower values of transmittance percentage due to the layer of grafted polyphenols[12] (Figure 6.2) mainly in the range 320–400 nm. B+P_S has a great alteration of the UV-Vis spectrum, caused by the variation of the glass lattice structure, upon irradiation, which is not related

to the grafted polyphenols.[34] The curve of B+P28 has a shape and values close to B, evidencing a reduction of the shielding effect which can be correlated with polyphenols release, as confirmed by the other tests. The significant decrease in reflectance/transmittance in the UV range observed for H+P and B+P a, can be associated with the shielding action of polyphenols in the UV range.[11] Flavonols and hydroxycinnamic acids, in fact, have UV screening properties: The first ones absorb the UV-A (approximately 320–400 nm) and the second ones absorb the UV-B radiations (approximately 280–320 nm)[35] as confirmed by the UV-Vis spectra of the functionalizing solution (Figure 1).

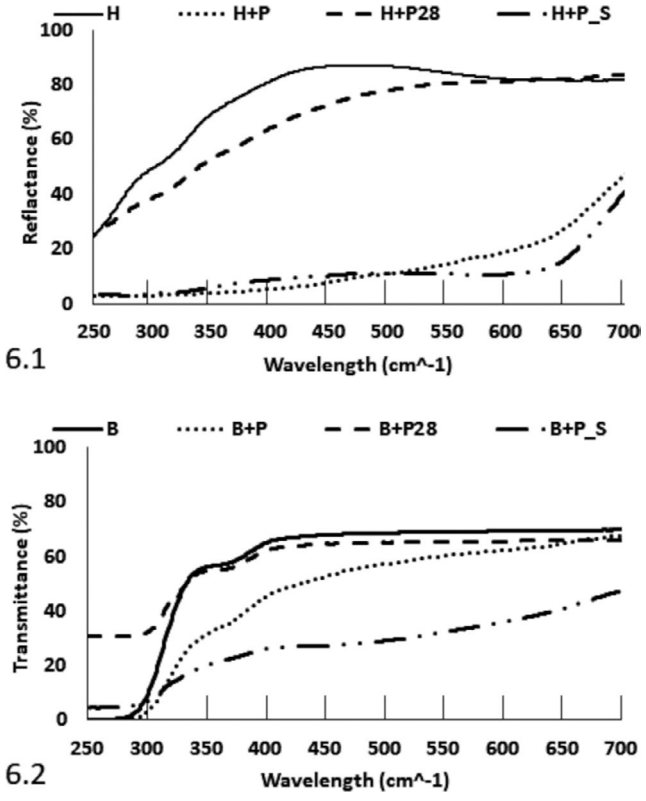

FIGURE 6 The reflectance spectra of hydroxyapatite and the transmittance spectra of SCNB through the use of UV-Vis spectroscopy. (6.1) Hydroxyapatite (H), functionalized hydroxyapatite (H+P), functionalized hydroxyapatite after the release test in water (H+P28) and functionalized hydroxyapatite after sterilization (H+P_S); (6.2) SCNB (B), functionalized SCNB (B+P), functionalized SCNB after the release test in water (B+P28), and functionalized SCNB after sterilization (B+P_S)

3.9 | XPS analysis of the extract and substrates (before and after functionalization)

The chemical composition of the freeze-dried extract of polyphenols (P) and of the surfaces before and after functionalization, as detected by XPS, is reported in Table 5.

The freeze-dried extract (P) is mainly constituted by C and O; Ca, N and P can be considered as contaminants. The surface of H is mainly constituted by O, Ca, and P, as expected for calcium phosphate. After polyphenols grafting (H+P), a significant increase in the carbon content can be observed as expected because of the presence of the grafted polyphenols. The surface of B is mainly constituted by O, Ca, Na, and Si, according to the glass composition. The high intensity of carbon can be ascribed to surface carbonation, as previously observed by the authors on bioactive glasses with high surface reactivity.[15,32] After polyphenols grafting, no increase in C is detectable (due to the high initial concentration of C), O slightly increases, Ca almost triples and P appears on the surface in low concentration, whereas Na decreases and Si disappears. XPS analyzes the outermost surface layer of a surface (penetration depth less than 10 nm) and suggests both for H+P and B+P an almost complete surface coverage by the polyphenols because the characteristic elements of the substrates are hidden after functionalization. The high-resolution spectra of C, O, and Ca are reported in Figure 7. The spectrum of Ca is absent for P because this element is negligible on that sample. Looking at H and B, three signals can be observed in the carbon region (Figure 7C) at 284.48–284.80, 285.52–285.76, and 288.76 eV. The first one, associated with the C–C and C–H bonds, and the second one, related to the C–O bond, can be ascribed to hydrocarbon contaminations from the atmosphere, always present onto reactive surfaces.[36,37] Finally, the signal at 288.48–288.76 eV can be associated with carbonates,[38] as expected.[15] In the oxygen region, two contributions are observed on H (Figure 7D) at 530.74 and 532.02 eV, which can be, respectively, associated with O in phosphates and hydroxyl groups.[39] Three contributions can be observed in the oxygen region of the B sample (Figure 7L): 531.21, 532.48 and 535.21 eV. The first one can be associated with the oxides in the glass network,[13] and the second one with OH and carbonates on the glass surface,[13,40] whereas the third one can be related to the Auger signal of Na.[40] Finally, two contributions are noted in the Ca region

TABLE 5 Surface chemical composition (at %) from the XPS survey analysis

	C	O	Ca	Ti	N	P	Na	Si	Mg
P	69	28.7	0.2	–	1.5	0.7	–	–	–
H	22	51.3	15.4	–	–	9.4	1.9	–	–
H+P	54.8	39.1	3.6	–	–	1.1	–	–	1.4
B	62	26.8	1.4	–	–	–	5.9	3.9	–
B+P	61.1	32.3	3.6	–	–	1.5	1.5	–	–

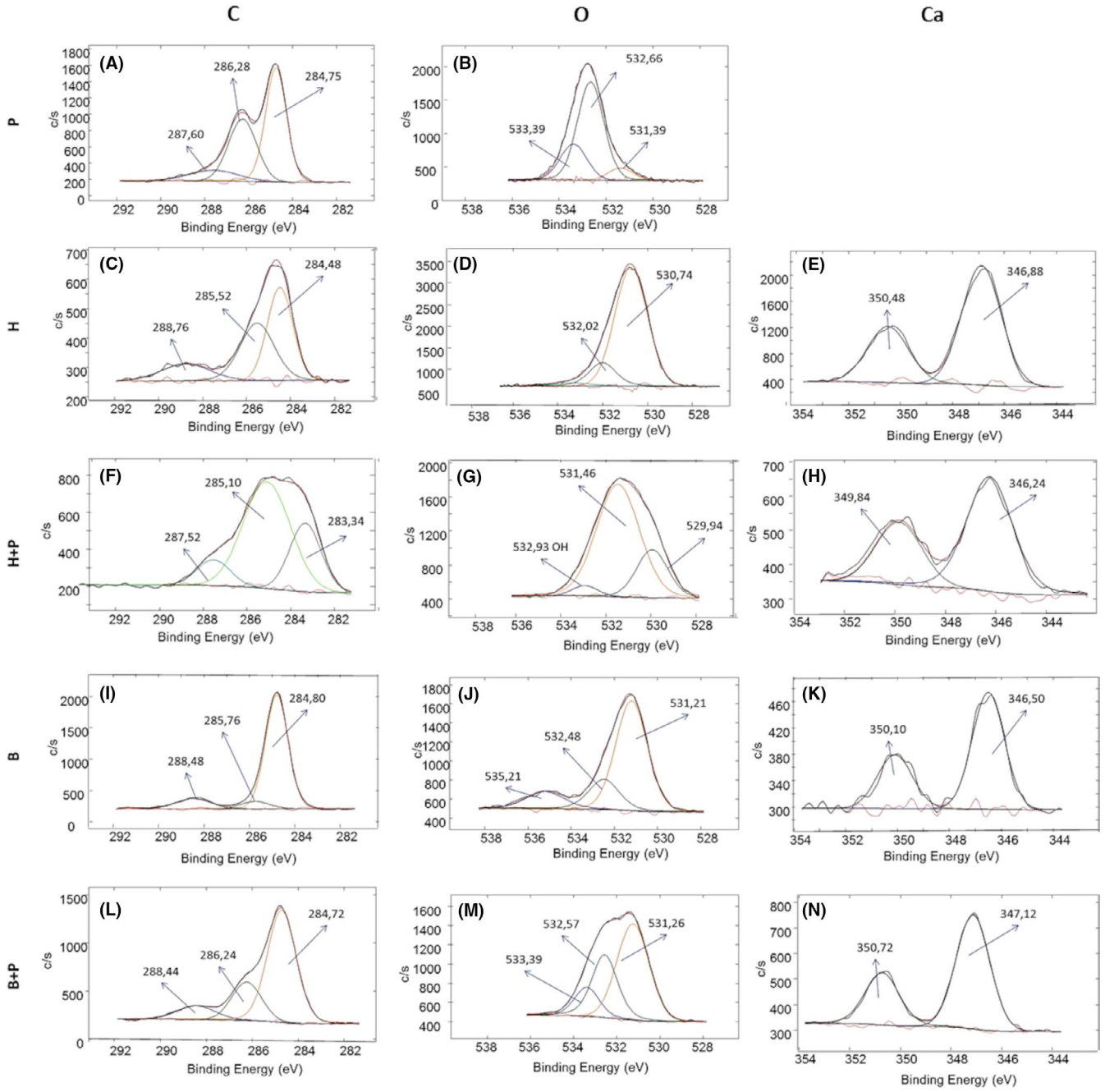

FIGURE 7 XPS high-resolution spectra for P (A, B), H (C, D, E), H+P (F, G, H), B (I, J, K), and B+P (L, M, N)

on the H sample at 348.88 and 350.48 eV, reported in the literature to be calcium phosphates of apatite.[39] Two signals can be noticed in the Ca region of the B sample (Figure 7M) at 346.50 and 350.10 eV. The signals can be associated with a calcium species with two peaks, Ca $2p_{3/2}$ and Ca $2p_{1/2}$ (spin-orbit splitting) in the bioactive glass. The spin-orbit split can be associated with calcium carbonate. Three main contributions can be evidenced in the carbon region for the sample P: 284.75, 286.28 and 287.60 eV can be, respectively, attributed to C–C or C–H, C–O, and C=O bonds.[36] Three contributions can be observed also in the oxygen region: 531.39, 532.66 and 533.39 eV, which can be, respectively, associated with the C–O, O=C–OH and aromatic OH groups.[36,37] Significant modifications of the high-resolution spectra of H and B surfaces are evidenced after polyphenols grafting (H+P and B+P). In the carbon region of H+P (Figure 7F), three contributions are observed: 283.34, 285.10 and 287.52 eV. The signal at 285.10 is associated with C–C and C–H bonds and the one at 287.52 to C=O bonds, as previously discussed for the extract of polyphenols.[36,37] The third signal is at lower binding energies usually associated with C bonds with metals, with possible presence also of oxygen, as reported in[41]

for Al-O-C or in[42] for Ti-C. In the oxygen region of H+P (Figure 7G), two main contributions can be noticed at 529.94 and 531.46 eV and a very low signal at 532.93 eV. The first one is associated with the C=O bond and the second one with the O=C–OH bond.[36,37] The third signal is associated with adsorbed water, because it is attributed to linked water, OH^- ions, or hydrogenophosphate.[43] Finally, a shift of the signals toward lower binding energies can be noticed in the calcium region with respect to the H reference sample. This shift is reported in literature concerning polyphenols-metal complexes.[44]

The high-resolution spectrum of the carbon region for the sample B+P (Figure 7N) evidenced three main contributions at 284.72, 286.24 and 288.44 eV, which can be associated with C–C/C–H, C–O, and carbonates.[36,38] The high-resolution spectrum of the oxygen region for B+P (Figure 7O) was similar to the one of the freeze-dried extract (Figure 7B): Three signals can be observed at 531.26, 532.57 and 533.39 eV and associated with C–O, O=C-OH, and aromatic OH,[36].[37] Finally, the high resolution of the calcium region (Figure 7P) has two signals at 347.12 and 350.72 eV, which are connected to the Ca–O bonds.[45] The high-resolution XPS spectra of the carbon and oxygen regions suggest some differences between H+P and B+P. The signal at about 283 eV, due to the bonding of carbon with metal ions,[36,37] is evident on H+P, but not on B+P. Moreover, the aromatic OH groups are clearly visible on B+P, as on the spectrum of the extract, but not on H+P. Finally, the high-resolution spectrum of Ca shows a shift of the peaks to lower energy for H+P and not for B+P (an opposite shift can be observed in this case). A decrease in the characteristic binding energies of the metal ions (Ca^{2+} ions) has been associated with the formation of complex compounds with polyphenols.[41]

XPS and zeta potential titration curves (Section 3.6) should be combined to have complementary information about the grafting mechanism. Zeta potential titration curve of H evidences high reactivity of H in an acidic liquid as it is in the functionalizing solution: The increase in the standard deviation of the zeta potential of H at pH lower than 4[46] is due to high surface reactivity and release of ions such as Ca^{2+}. The released Ca^{2+} ions form a bond with the phenolic groups of the polyphenols (which are completely deprotonated at pH 6 as showed by the zeta potential titration curve of the functionalizing solution) and with the surface of H, acting as mediators of grafting. The bond between the Ca^{2+} ions and the surface of H can occur through electrostatic attraction by the hydroxyl groups of the H surface which are completely dissociated at pH higher than 5.5 (as showed by the plateau in the zeta potential titration curve of H) that is the pH value of the Uptake H during the functionalization process. This kind of grafting has been previously observed by the authors on chemically treated titanium surfaces.[47] In that case, the Ca^{2+} ions were added into the functionalization solution, whereas in the case of hydroxyapatite, the Ca^{2+} ions are released by the substrate during the functionalization process, these form complex compounds with the polyphenols in the solution which mediate the grafting mechanism to the surface.

Concerning B (Figure 4.2), a different mechanism of grafting can be supposed. In this case, functionalization occurs at pH 3.6–4.6 and polyphenols have deprotonated carboxylic groups (not the phenolic ones) and the B surface has protonated OH groups. In this case, grafting occurs without the Ca^{2+} ions as mediators. A high surface chemical reactivity at alkaline pH is highlighted for B by the zeta potential titration curve, as expected for reactive silica-based materials.[48] This phenomenon is attenuated on B+P (standard deviation values very low in the basic range), because of the presence of the polyphenols, which cover and protect the surface, exercising a shielding effect, able to reduce the reactivity of the surface itself. This behavior suggests that the grafted polyphenols are stable in the explored basic environment. On the contrary, the standard deviation of the zeta potential values increases in the acidic range for the B+P sample: This can be due to the instability of the grafted polyphenols at pH lower than 4, when their carboxylic groups, which are involved in the bond with the surface, are protonated. A release of the grafted polyphenols at this pH value can be hypothesized for this biomaterial.

Looking at the main results of the research, it can be assessed that the extract of organic red grape pomace used in this research contains monomer flavan-3-ols and condensed tannins with a high percentage of (−)-epicatechin and a moderate polymerization degree (mDP), as well as hydroxycinnamic acids. When the freeze-dried extract is solved into ultra-pure water (functionalization solution), it has an acidic pH and condensed tannins with a lower mDP. The condensed tannins grafted on the surfaces have a similar mDP as those in the solution, but a higher percentage of (+)-catechin: The grafted biomolecules are known to be active both for protection and formation of biological tissues and it will be of interest to study these functionalized surfaces in a biological environment. The functionalization process is effective on H and B and it does not degrade polyphenols. There is a difference in the amount of the grafted polyphenols on the explored substrates: A significant amount is grafted on hydroxyapatite and bioactive glass B (higher surface reactivity), whereas it is almost undetectable on bioactive glass A (low surface reactivity because of the alumina content). Grafting does not inhibit the chemical redox and radical scavenging ability of polyphenols. The grafted polyphenols make a continuous layer, but big agglomerates are also detected on bioactive glass B. There is a different grafting mechanism of polyphenols on H and B. It occurs through the mediation of Ca^{2+} ions and the phenolic groups of polyphenols in the case of H, whereas it occurs through the carboxylic groups of polyphenols and the OH groups exposed by the surface of the substrate, in the case of bioactive glass B. The released

polyphenols maintain their redox chemical reactivity and a homogeneous thin surface layer of polyphenols is still firmly grafted on both the substrates after 28 days of soaking and it still has radical scavenging activity. Finally, the functionalized samples can be sterilized by gamma radiation that is a crucial prerequisite for the clinical application of a new biomaterial.

The effects of the grafted polyphenols in terms of biological response are not here investigated, but in the light of the obtained results both an early (due to polyphenols release) and long-lasting (due to the firmly grafted polyphenols) beneficial effect can be expected in terms of osteogenic stimulation and anti-inflammatory properties.

4 | CONCLUSIONS

This paper gives a new insight into the advantages of bioceramics, such as hydroxyapatite, and bioglasses as implant surfaces. The results suggest that polyphenols extracted from red grape pomaces can be effectively grafted on hydroxyapatite and bioactive glasses, if the glass is properly selected in order to have sufficient surface reactivity. The grafting mechanism depends on the substrate characteristics and can involve Ca^{2+} ions as mediators. Grafted polyphenols maintain their redox and radical scavenging activity, can be sterilized by gamma irradiation, and are released in water up to 28 days. However, after the release test, an active thin layer of molecules is still present on the surface. In conclusion, this functionalization route appears promising for the development of multifunctional and sustainable innovative biomaterials for bone regeneration. The next step of this research will be the characterization of the functionalized surfaces in a biological environment.

ACKNOWLEDGMENTS

The European Commission and the National Agencies (MIUR, The Icelandic Technology Development Fund) are acknowledged for funding the project NAT4MORE within the call M.ERA-NET Joint Call 2016 (Reference Number: project 4169). The DIMEAS Department of Politecnico di Torino is kindly acknowledged for supporting the freeze-drying process of the extract. The Department of Drug Science and Technology of Università di Torino is kindly acknowledged for the zeta potential curves measurements of the functionalizing solution. INTRAUMA is acknowledged to provide the sterilization of functionalized samples.

ORCID

Giacomo Riccucci https://orcid.org/0000-0001-6127-2147
Marta Miola https://orcid.org/0000-0002-1440-6146
Enrica Verné https://orcid.org/0000-0002-8649-4739
Silvia Spriano https://orcid.org/0000-0002-7367-9777

REFERENCES

1. Hench LL. Bioceramics. J Am Ceram Soc. 1998;81(7):1705–28.
2. Fiume E, Barberi J, Verné E, Baino F. Bioactive glasses: from parent 45S5 composition to scaffold-assisted tissue-healing therapies. J Funct Biomater. 2018;9(1).
3. Baino F, Hamzehlou S, Kargozar S. Bioactive glasses: where are we and where are we going? J Funct Biomater. 2018;9(25):25.
4. Ko C-L, Chen W-C, Chen J-C, Wang Y-H, Shih C-J, Tyan Y-C, et al. Properties of osteoconductive biomaterials: calcium phosphate cement with different ratios of platelet-rich plasma as identifiers. Mater Sci Eng C. 2013;33(6):3537–44.
5. Kaneko A, Marukawa E, Harada H. Hydroxyapatite nanoparticles as injectable bone substitute material in a vertical bone augmentation model. Vivo. 2020;34(3):1053–61.
6. Torre E, Iviglia G, Cassinelli C, Morra M, Russo N. Polyphenols from grape pomace induce osteogenic differentiation in mesenchymal stem cells. Int J Mol Med. 2020;45(6):1721–34.
7. Gómez-Florit M, Monjo M, Ramis JM. Identification of quercitrin as a potential therapeutic agent for periodontal applications. J Periodontol. 2014;85(7):966–74.
8. Byun MR, Sung MK, Kim AR, Lee CH, Jang EJ, Jeong MG, et al. Epicatechin gallate (ECG) stimulates osteoblast differentiation via runt-related transcription factor 2 (RUNX2) and transcriptional coactivator with PDZ-binding motif (TAZ)-mediated transcriptional activation. J Biol Chem. 2014;289(14):9926–35.
9. Guaita M, Bosso A. Polyphenolic characterization of grape skins and seeds of four Italian red cultivars at harvest and after fermentative maceration. Foods. 2019;8(9):395.
10. Venturelli S, Burkard M, Biendl M, Lauer UM, Frank J, Busch C. Prenylated chalcones and flavonoids for the prevention and treatment of cancer. Nutrition. 2016;32(11–12):1171–8.
11. Verné E, Ferraris S, Vitale-Brovarone C, Spriano S, Bianchi CL, Naldoni A, et al. Alkaline phosphatase grafting on bioactive glasses and glass ceramics. Acta Biomater. 2010;6(1):229–40.
12. Zhang X, Ferraris S, Prenesti E, Verné E. Surface functionalization of bioactive glasses with natural molecules of biological significance, Part I: gallic acid as model molecule. Appl Surf Sci. 2013;287:329–40.
13. Verné E, Vitale-Brovarone C, Bui E, Bianchi CL, Boccaccini AR. Surface functionalization of bioactive glasses. J Biomed Mater Res - Part A. 2009;90(4):981–92.
14. Bosso A, Guaita M, Petrozziello M. Influence of solvents on the composition of condensed tannins in grape pomace seed extracts. Food Chem. 2016;207:162–9.
15. Cazzola M, Corazzari I, Prenesti E, Bertone E, Verné E, Ferraris S. Bioactive glass coupling with natural polyphenols: surface modification, bioactivity and anti-oxidant ability. Appl Surf Sci. 2016;30(367):237–48.
16. Rajbhar K, Dawda H, Mukundan U. Polyphenols: methods of extraction. Sci Rev Chem Commun. 2015;5(1):1–6.
17. Di Stefano R, Cravero MC. Metodi per lo studio dei polifenoli dell'uva. Riv di Enol e Vitic. 1989;2:83–9.
18. Kennedy JA, Jones GP. Analysis of proanthocyanidin cleavage products following acid-catalysis in the presence of excess phloroglucinol. J Agric Food Chem. 2001;49(4):1740–6.
19. Ducasse MA, Canal-Llauberes RM, de Lumley M, Williams P, Souquet JM, Fulcrand H, et al. Effect of macerating enzyme

treatment on the polyphenol and polysaccharide composition of red wines. Food Chem. 2010;118(2):369–76.
20. Ferraris S, Zhang X, Prenesti E, Corazzari I, Turci F, Tomatis M, et al. Gallic acid grafting to a ferrimagnetic bioactive glass-ceramic. J Non Cryst Solids. 2016;432:167–75.
21. Ignat I, Volf I, Popa VI. A critical review of methods for characterisation of polyphenolic compounds in fruits and vegetables. Food Chem. 2011;126(4):1821–35.
22. Aleixandre-Tudo JL, du Toit W. The role of UV-visible spectroscopy for phenolic compounds quantification in winemaking. Front New Trends Sci Ferme Food Bever. 2016;1–21. Available from: https://www.researchgate.net/publication/330938879_The_Role_of_UV-Visible_Spectroscopy_for_Phenolic_Compounds_Quantification_in_Winemaking. Accessed 20 May 2021.
23. Fidelis M, Santos JS, Coelho ALK, Rodionova OY, Pomerantsev A, Granato D. Authentication of juices from antioxidant and chemical perspectives: a feasibility quality control study using chemometrics. Food Control. 2017;1(73):796–805.
24. Mishra K, Ojha H, Chaudhury NK. Estimation of antiradical properties of antioxidants using DPPH assay: a critical review and results. Food Chem. 2012;130(4):1036–43.
25. Lavid N, Schwartz A, Yarden O, Tel-Or E. The involvement of polyphenols and peroxidase activities in heavy-metal accumulation by epidermal glands of the waterlily (nymphaeaceae). Planta. 2001;212:323–31.
26. Talamond P, Verdeil JL, Conéjéro G. Secondary metabolite localization by autofluorescence in living plant cells. Molecules. 2015;20(3):5024–37.
27. Souquet J, Cheyner VIR, Brossaud F, Moutounet M. Polymeric proanthocyanidins from grape skins. Phytochemistry. 1996;43(2):509–12.
28. Tsuchiya H. Stereospecificity in membrane effects of catechins. Chem Biol Interact. 2001;134(1):41–54.
29. Harnly JM, Bhagwat S, Lin LZ. Profiling methods for the determination of phenolic compounds in foods and dietary supplements. Anal Bioanal Chem. 2007;389(1):47–61.
30. Kong KW, Mat-Junit S, Ismail A, Aminudin N, Abdul-Aziz A. Polyphenols in Barringtonia racemosa and their protection against oxidation of LDL, serum and haemoglobin. Food Chem. 2014;146:85–93.
31. Cerruti M, Morterra C. Carbonate formation on bioactive glasses. Langmuir. 2004;20:6382–8.
32. Ferraris S, Miola M, Cochis A, Azzimonti B, Rimondini L, Prenesti E, et al. In situ reduction of antibacterial silver ions to metallic silver nanoparticles on bioactive glasses functionalized with polyphenols. Appl Surf Sci. 2017;396:461–70.
33. Singh BP, Menchavez R, Takai C, Fuji M, Takahashi M. Stability of dispersions of colloidal alumina particles in aqueous suspensions. J Colloid Interface Sci. 2005;291(1):181–6.
34. Farag MM, Abd-Allah WM, Ahmed HYA. Study of the dual effect of gamma irradiation and strontium substitution on bioactivity, cytotoxicity, and antimicrobial properties of 45S5 bioglass. J Biomed Mater Res A. 2017;105A(6):1646–55.
35. Kolb CA, Kopeck J, Riederer M, Pfündel EE. UV screening by phenolics in berries of grapevine (Vitis vinifera). Funct Plant Biol. 2003;30:1177–86.
36. Neo YP, Swift S, Ray S, Gizdavic-Nikolaidis M, Jin J, Perera CO. Evaluation of gallic acid loaded zein sub-micron electrospun fibre mats as novel active packaging materials. Food Chem. 2013;141(3):3192–200.
37. Lee HP, Lin DJ, Yeh ML. Phenolic modified ceramic coating on biodegradable Mg alloy: the improved corrosion resistance and osteoblast-like cell activity. Materials (Basel). 2017;10(7).
38. X-ray photoelectron spectroscopy (XPS) reference pages. Available from: http://www.xpsfitting.com/2011/03/c-1s-carbonates.html. Accessed 26 Apr 2021.
39. Gomes GC, Borghi FF, Ospina RO, López EO, Borges FO, Mello A. Nd: YAG (532 nm) pulsed laser deposition produces crystalline hydroxyapatite thin coatings at room temperature. Surf Coatings Technol. 2017;329:174–83.
40. XPS reference table of elements, oxygen. Available from: https://xpssimplified.com/elements/oxygen.php. Accessed 26 Apr 2021.
41. de Riccardis MF. Formation of nanolayer on surface of EPD coatings based on poly-ether-ether-ketone. Intech. 2017;3–26. Available from: https://www.intechopen.com/books/nanoscaled-films-and-layers/formation-of-nanolayer-on-surface-of-epd-coatings-based-on-poly-ether-ether-ketone
42. Yang H, Jiang L, Li Y, Li G, Yang Y, He J, et al. Highly efficient red cabbage anthocyanin inserted TiO2 aerogel nanocomposites for photocatalytic reduction of Cr (VI) under visible light. Nanomaterials. 2018;8(937):1–15.
43. Maachou H, Genet MJ, Aliouche D, Dupont-gillain CC, Rouxhet PG. XPS analysis of chitosan–hydroxyapatite biomaterials: from elements to compounds. Surf Interface Anal. 2013;45:1088–97.
44. Zhang H, Xie L, Shen X, Shang T, Luo R, Li X, et al. Catechol/polyethyleneimine conversion coating with enhanced corrosion protection of magnesium alloys: potential applications for vascular implants. J Mater Chem B. 2018;6(43):6936–49.
45. Ferreira FV, Souza LP, Martins TMM, Lopes JH, Mattos BD, Mariano M, et al. Electronic supplementary information nanocellulose/bioactive glass cryogels as scaffolds for bone regeneration. R Soc Chem. 2019;1–24.
46. Mera AC, Contreras D, Escalona N, Mansilla HD. BiOI microspheres for photocatalytic degradation of gallic acid. J Photochem Photobiol A Chem. 2016;318:71–6.
47. Cazzola M, Ferraris S, Prenesti E, Casalegno V, Spriano S. Grafting of Gallic acid onto a bioactive ti6al4v alloy: a physicochemical characterization. Coating. 2019;9(302):1–17.
48. Frankel GS, Vienna JD, Lian J, Scully JR, Gin S, Ryan JV, et al. A comparative review of the aqueous corrosion of glasses, crystalline ceramics, and metals. Nat Partn Journals. 2018;15(1):1–17.

SUPPORTING INFORMATION

Additional supporting information may be found online in the Supporting Information section.

How to cite this article: Riccucci G, Cazzola M, Ferraris S, et al. Surface functionalization of bioactive glasses and hydroxyapatite with polyphenols from organic red grape pomace. *J Am Ceram Soc*. 2022;105:1697–1710. https://doi.org/10.1111/jace.17849